SAND2021-9836C

Cost-Effective Measurement of Surface Radiative Properties for Simulation Uncertainty Quantification (UQ) Analysis

Rebekah L. Travis, Karen N. Son

Abstract

This poster describes how experimental measurements of surface radiative properties were used to improve thermal simulation predictions and quantify model uncertainty. A systematic approach is presented leveraging both low-cost and high-fidelity reflectometers to achieve maximum model accuracy with minimal cost and effort. Two finite element models (FEM) are used to demonstrate this approach and illustrate the importance of measuring surface radiative properties for accurate simulation predictions.

Background

Accurate data on the emittance of materials is critical for calculating radiative heat transfer in coupled simulations of systems. The current industry standard for measuring emittance is done indirectly through a hemispherical directional reflectometer (HDR), where the emittance of an opaque sample is determined using measurements of reflectance and Kirchhoff's law: [1].

For gray irradiation and/or diffuse radiation:

$$\varepsilon_\lambda(T,\lambda) = \alpha_\lambda(T,\lambda) = 1 - \rho_\lambda(T,\lambda)$$

T, absolute temperature of body in Kelvin
λ, wavelength of radiation
ε_λ, emissivity
ρ_λ, reflectivity
α_λ, absorptivity

HDRs are benchtop instruments that require substantial time to use—approximately 4 hours per sample compared to 2 minutes to measure a sample with a handheld meter.

Benchtop Instrumentation

Measurements of infrared spectral HDR from 2.0 to 25.0 µm were performed with a Thermo Scientific™ Nicolet™ 5700 Fourier transform infrared (FTIR) Spectrometer coupled to a SOC-100 HDR Hemispherical Directional Reflectometer accessory from Surface Optics Corporation (SOC) [2-5]. An Agilent Cary 5000 UV/VIS/NIR spectrophotometer was also used and measured reflectances from 0.2 to 2.5 µm.

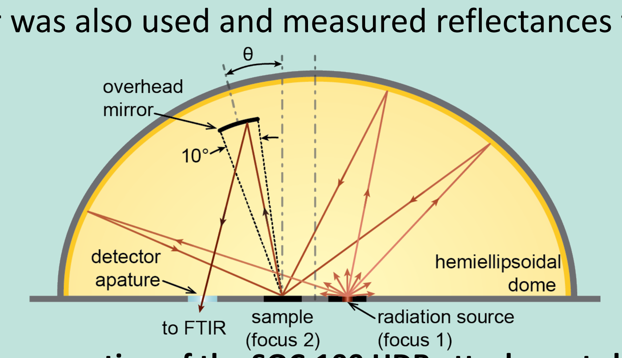

Fig 1. Schematic cross section of the SOC-100 HDR attachment showing the sample, radiation source, overhead mirror, and detector aperture

Handheld Instrumentation

The SOC 410-Solar measures total reflectance across seven sub-bands in the 0.335 µm to 2.5 µm (335 nm to 2500 nm) spectral regions. The 410-Solar uses a modified integrating sphere that is equipped with a shutter called a beam blocker to measure diffuse and specular reflectance.

The ET-100 measures directional reflectance across six bands in the thermal infrared spectral region . Light from the source scatters off of the sample into the integrating sphere, where it bounces around until it is absorbed by the sample or gold coated sphere, or passes through the detector baffles. After completing the first measurement at 20° incident angles, the illuminating source rotates, and the process is repeated for a 60° incident angle [6].

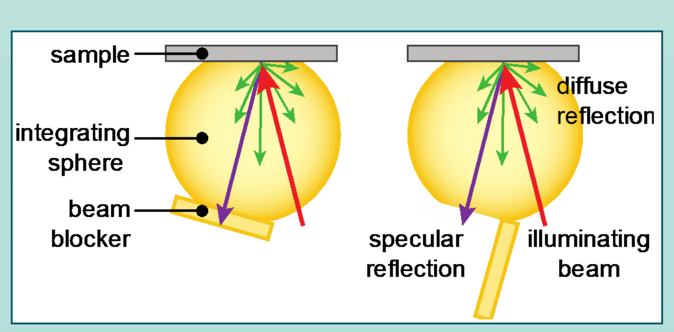

Fig. 2 – Schematic of the SOC 410-Solar optical system showing beam blocker functionality. Integrating sphere with beam blocker (left) closed and (right) open

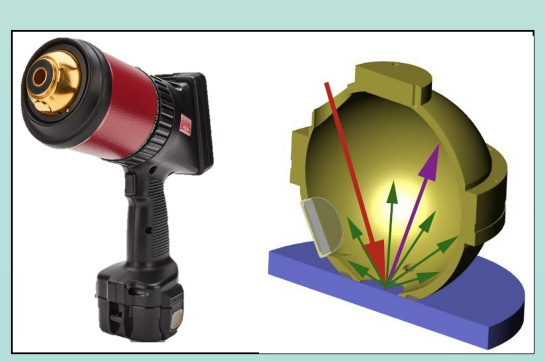

Fig. 3 – (Left) photograph of the ET-100 handheld meter, and (Right) schematic of the integrating sphere. Red arrow – illuminating beam; purple arrow – reflected beam; green arrows – scattered light. Images from [6]

Experimentation

Thermal Soak Test

The Thermal Soak test is an environmental test design to gather thermal performance data of the shipping container in a representative normal thermal environment for 7 days. The shipping container was placed in an open parking lot of Sandia National Laboratories in Albuquerque, New Mexico and instrumented with 51 thermocouples located on the interior and 28 thermocouples on the exterior of the container. Local solar and weather data were used to derive the boundary conditions for the simulations.

Experimentally Derived Emissivity Values

The initial surface radiative properties of materials input into the thermal soak simulations came from a literature search for soiled white paint [KNS]. After discovering a large deviation between experimental and simulation results, both the handheld and benchtop tools were used to experimentally determine the emissivity and absorptivity values of various materials of the shipping container. Special attention was paid to the exterior of the container, made of white painted aluminum, but slight differences exist between the sides. The top had a significant level of dust/dirt accumulation compared to the front and sides. Measurements were taken both before (dirty) and after cleaning the exterior with alcohol. The dust/dirt accumulation had little effect on the emissivity values but a more significant effect on the absorptivity, and thus the reflectivity values. The emissivity and absorptivity measurements were then input into a new set of simulations.

The materials studied had good agreement between handheld and benchtop emittance measurements because of their composition. There are classes of materials and surface treatments where this assumption breaks down. For example, samples that have a high degree of surface topology like those from additive manufacturing have strong directional dependencies [7] that will not be captured by a handheld unit. Other more exotic samples like photonic crystals [8], metasurfaces [9], nanostructured films [10], and gratings [11] have dispersion characteristics that require the use of the benchtop instruments that can resolve different polarizations and directions.

Table 1 – Number of measurements taken on each material with each tool

Surface Description	ET-100	SOC-410	HDR
White Painted Aluminum	152	699	2
Unpainted, Brushed Aluminum	6	–	–
Mill Finished Aluminum, 5052-H3	21	–	–
Brushed Aluminum, Coarse ~60-80 grit	12	–	–
Electroless Nickel-plated Aluminum	35	–	–
Mill Finished Aluminum 6061-T6 & CNC End Milled Aluminum 6061-T6	15	–	–
Brushed Stainless Steel, Coarse ~80-100 grit	10	15	–

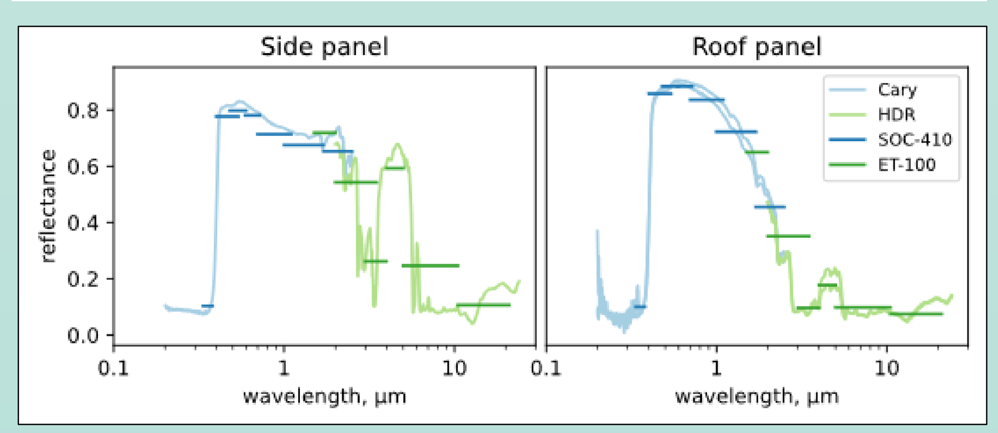

Fig. 4 – Comparison of the spectral reflectance measurements from the benchtop and handheld measurements

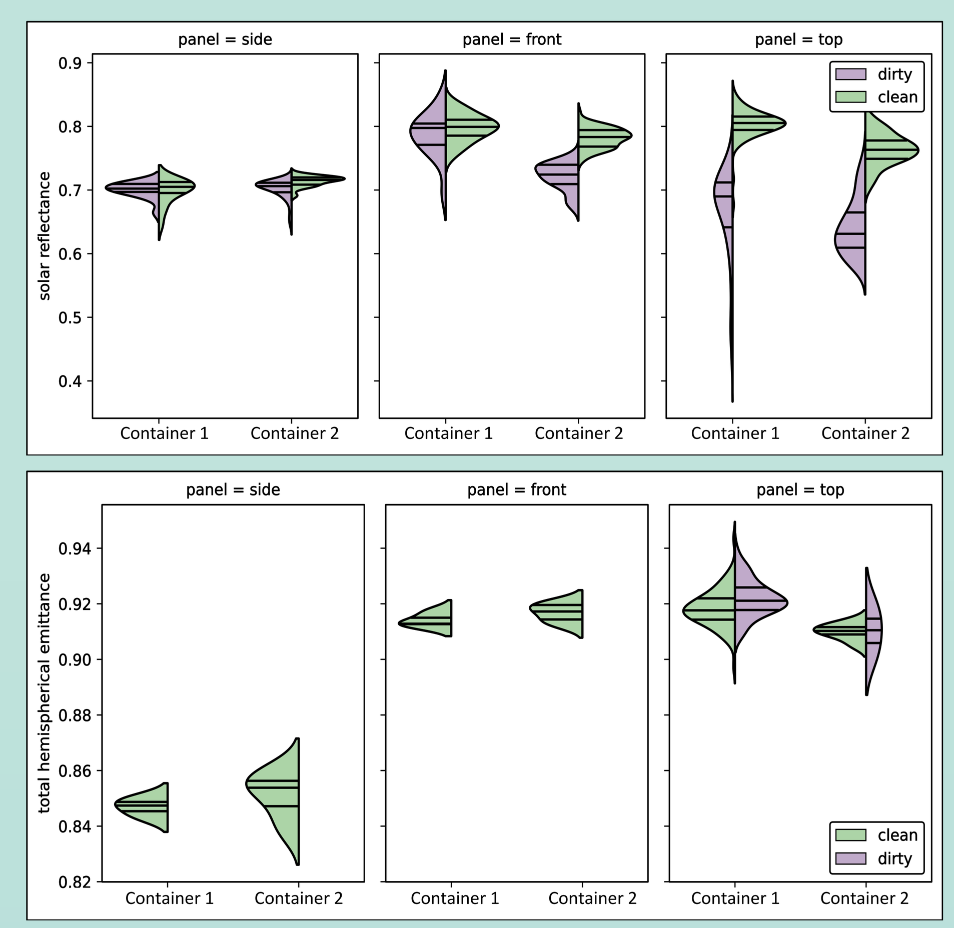

Fig. 5 – (Top) Violin plot of solar reflectivity measurements on the container exterior grouped by treatment; (Bottom) Violin plot of HTE measurements on the container exterior grouped by treatment

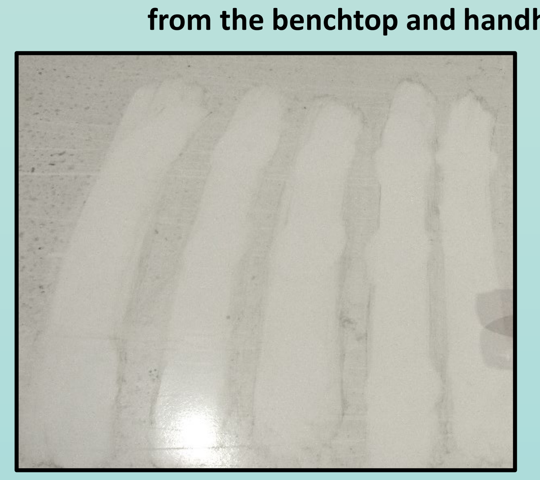

Fig. 6 – Photograph on the top of the container after spot cleaning to measure with the ET-100 and 410-Solar

Table 2 – Assumed versus measured emissivity values for the exterior sides of the container

Location	ε Assumed Values	ε Measured Values
Side of Container	0.4	0.85
Top of Container	0.4	0.919
Front of Container	0.4	0.919
Bottom of Container	0.888	0.931
Rear of Container	0.285	0.171

Table 3 – Assumed versus measured absorptivity values for the exterior sides of the container

Location	α Assumed Values	α Measured Values
Side of Container	0.4	0.299
Top of Container	0.25	0.348
Front of Container	0.4	0.268
Bottom of Container	0.4	0.741
Rear of Container	0.4	0.496

Model Validation Results

There is a more apparent difference in temperatures with the measured emissivity values for the interior of the container compared to the exterior of the container. High frequency fluctuations can be seen on the exterior wall data as the exterior wall is more directly affected by the solar irradiation. As the energy passes through the wall materials, the wall effectively acts as a low pass filter, smoothing the data thus making the difference in temperatures more apparent for the interior wall.
The average difference between experimental and computational results decreases from multiple degrees to less than a degree when the experimental emissivity values were used as an input, showing an increase in model integrity.

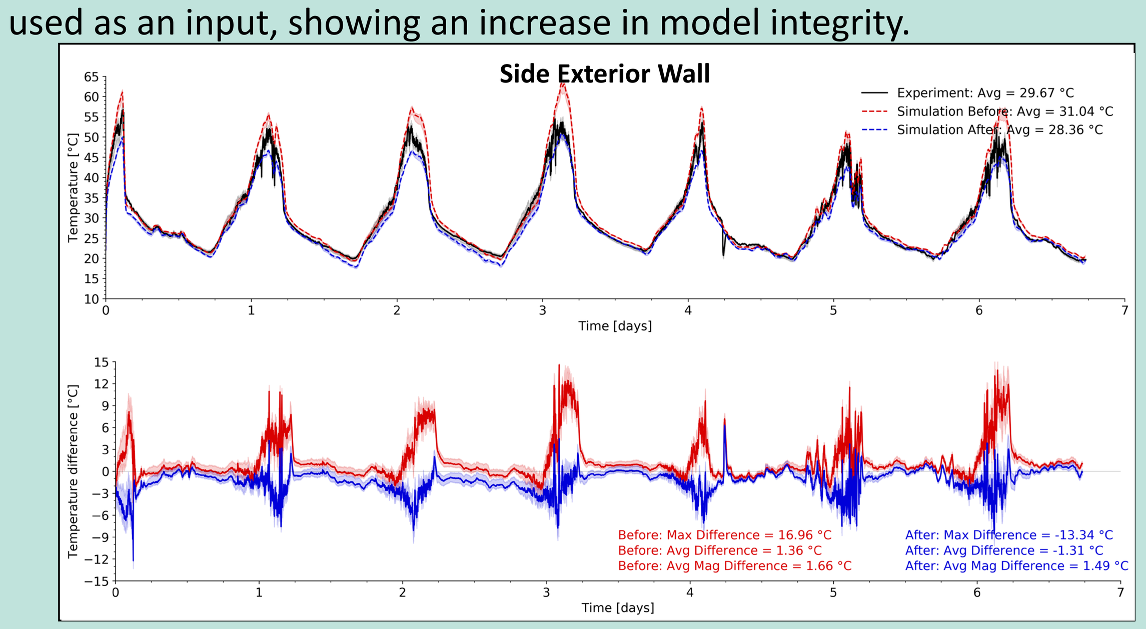

Fig. 7 – Side exterior wall (Top) simulation temperatures before and after experimental radiative properties were measured compared to experimental temperatures; (Bottom) difference in simulation and experimental temperatures

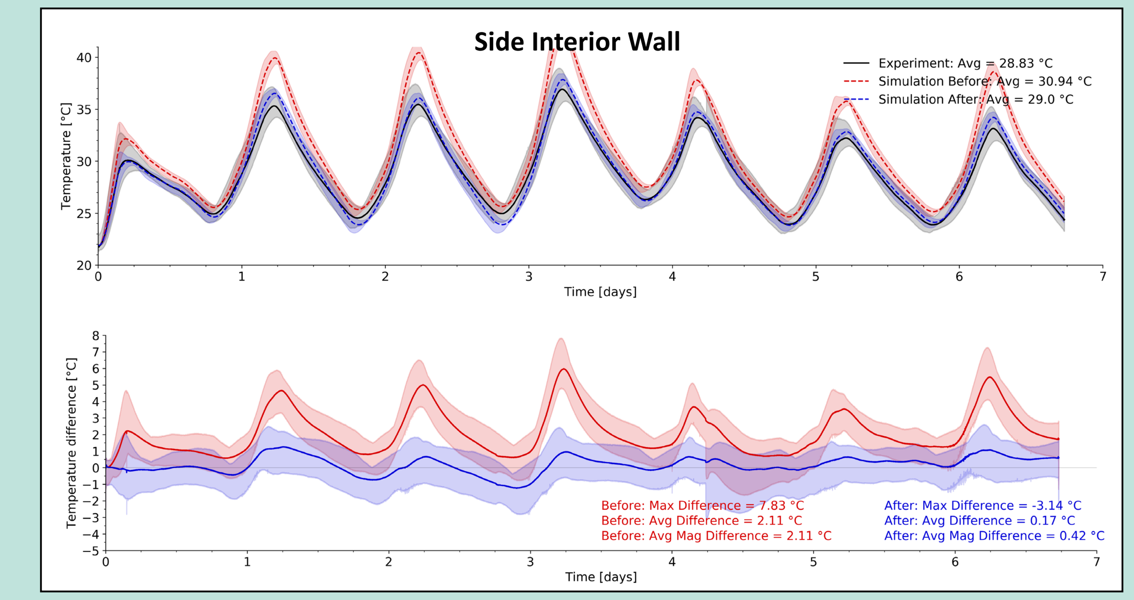

Fig. 8 – Side interior wall (Top) simulation temperatures before and after experimental radiative properties were measured compared to experimental temperatures; (Bottom) difference in simulation and experimental temperatures

Conclusions

- There are discrepancies between measured values and historical emittance values used in models, which can be diminished by experimental measurements
- Comparison of benchtop to handheld measurements indicate that handheld instruments can adequately measure surface properties on the present materials.
- Surface contamination (i.e., cleanliness) has a large effect on solar reflectance with dirty panels absorbing more solar irradiation thus heating up faster, but does not affect the emittance in the IR range.

References

[1] F. Incropera, D. Dewitt, T. Bergman, and A. Lavine. *Introduction to Heat Transfer.* United States of America: John Wiley and Sons, 2007.
[2] A. R. Ellis, H. M. Graham, M. B. Sinclair, and J. C. Verley, "Variable-angle directional emissometer for moderate-temperature emissivity measurements.," Sandia National Lab. (SNL-NM), Albuquerque, NM (United States), SAND2008-4043C, Aug. 2008. Accessed: Nov. 11, 2020. [Online]. Available: https://www.osti.gov/biblio/1272591.
[3] J. T. Neu, M. T. Beecroft, and R. Schramm, "Extended performance infrared directional reflectometer for the measurement of total, diffuse, and specular reflectance," in *Stray Radiation in Optical Systems III*, Oct. 1994, vol. 2260, pp. 62–73, doi: 10.1117/12.189204.
[4] H. M. Graham and H. G. C. Jr, "Correction for angular spread in HDR determination of IR optical constants," in *Optical Diagnostic Methods for Inorganic Materials III*, Nov. 2003, vol. 5192, pp. 80–90, doi: 10.1117/12.505322.
[5] "Lab Reflectometer SOC-100 HDR." https://surfaceoptics.com/products/reflectometers-emissometers/soc-100-hdr/ (accessed Nov. 11, 2020).
[6] "ET100 Emissometer." https://surfaceoptics.com/products/reflectometers-emissometers/et100-thermal-hand-held-emissometer/ (accessed Nov. 11, 2020).
[7] S. Taylor, J. B. Wright, E. C. Forrest, B. Jared, J. Koepke, and J. Beaman, "Investigating relationship between surface topography and emissivity of metallic additively manufactured parts," *Int. Commun. Heat Mass Transf.*, vol. 115, p. 104614, Jun. 2020, doi: 10.1016/j.icheatmasstransfer.2020.104614.
[KNS] F. Kreith and J. Kreider, Principles of Solar Engineering. 2000. doi: 10.1201/b18119.
[8] S. Noda, "Thermal emission control by photonic crystals," in *2016 21st OptoElectronics and Communications Conference (OECC) held jointly with 2016 International Conference on Photonics in Switching (PS)*, Jul. 2016, pp. 1–1.
[9] D. Costantini *et al.*, "Plasmonic Metasurface for Directional and Frequency-Selective Thermal Emission," *Phys. Rev. Appl.*, vol. 4, no. 1, p. 014023, Jul. 2015, doi: 10.1103/PhysRevApplied.4.014023.
[10] D. B. Burckel, P. S. Davids, P. S. Finnegan, P. N. Figueiredo, and J. C. Ginn, "Directional emissivity from two-dimensional infrared waveguide arrays," *Appl. Phys. Lett.*, vol. 107, no. 12, p. 121902, Sep. 2015, doi: 10.1063/1.4931124.
[11] J. Le Gall, M. Olivier, and J.-J. Greffet, "Experimental and theoretical study of reflection and coherent thermal emissionby a SiC grating supporting a surface-phonon polariton," *Phys. Rev. B*, vol. 55, no. 15, pp. 10105–10114, Apr. 1997, doi: 10.1103/PhysRevB.55.10105.

Sandia National Laboratories is a multimission laboratory managed and operated by National Technology &Engineering Solutions of Sandia, LLC, a wholly owned subsidiary of Honeywell International Inc., for the U.S. Department of Energy's National Nuclear Security Administration under contract DE-NA0003525.
SAND No. ____________

Sandia National Laboratories is a multimission laboratory managed and operated by National Technology & Engineering Solutions of Sandia, LLC, a wholly owned subsidiary of Honeywell International Inc., for the U.S. Department of Energy's National Nuclear Security Administration under contract DE-NA0003525.